J. Fluid Mech. (1980), *vol.* 97, *part* 1, *pp.* 91–114
Printed in Great Britain

The tank wall effect on internal waves due to a transient vertical force moving at fixed depth in a density-stratified fluid

By E. W. GRAHAM AND B. B. GRAHAM
Graham Associates, Shaw Island, WA. 98286

(Received 27 November 1978 and in revised form 24 April 1979)

The fluid is incompressible, inviscid and non-diffusive. It has a uniform Brunt–Väisälä frequency, N, and is of constant depth, D. A body or wing moves horizontally through the fluid at velocity U in a straight line, exerting a vertical force during a given time interval. The force is constant, or oscillatory with frequency σ. The vertical average of the strain rate in a thin surface layer is calculated for a network of points behind the body.

The linearized analysis is first applied with tank walls, then modified for remote walls and a vertical force of long duration.

For moderately high velocity and forcing frequency ($U/ND = 5$, $\sigma/N \cong 4$–16) the recurring internal wave pattern just behind the body is well established in one cycle of the oscillatory force. A tank width one or two times the depth gives good agreement between tank and no-wall calculations for the chosen examples.

For a stationary wing ($U/ND = 0$) in a cubic tank with forcing frequency one-half the natural frequency ($\sigma/N = \frac{1}{2}$) the strain rates after one cycle are 10^3 times greater than for the moving wing case. After five cycles the magnitudes are twenty times larger than after one cycle. Presumably these large increases are due to the continuous and efficient feeding of energy into a small fluid volume which occurs for the stationary wing. No-wall calculations for many cycles give amplitudes roughly one-half those for five cycles in the tank, showing the effect of escaping energy.

The relation of these developments to stationary phase analysis and preferred directions is discussed.

1. Introduction

A body in steady or transient motion through a density-stratified fluid produces internal waves. Such waves may, for example, be created by the volume of the body displacing fluid, which by continuity must flow from the new position of the body to fill in the position vacated. Such flow generally involves vertical fluid motion with consequent disturbance of the equilibrium stratification. Even in the absence of volume effects rigid surfaces may exert forces on the fluid which disturb the equilibrium stratification, and produce restoring forces (in stably stratified fluid) and internal waves. The wake behind the body, through its turbulent motion and collapse, may also cause internal waves.

Here we consider the effect of a transient lift† (vertical force) which is exerted by the

† The stipulation of a rigid body in fluctuating motion leads to a much more difficult analysis.

0022-1120/80/4391-8380 $02.00

body on the fluid only during the time interval from $t' = 0$ to $t' = \tau$. This lift may be constant during that time interval or vary from plus to minus (upwards to downwards) in simple harmonic fashion. The latter case might correspond to a horizontally moving body oscillating in pitch in a quiescent fluid or to a steadily moving body in a background field of internal waves.

A related problem considered by Rehm & Radt (1975) is the production of internal waves by a body which moves horizontally at uniform speed but with superimposed 'heaving' oscillations. They considered a constant Brunt–Väisälä frequency (N) and infinite depth. In the heaving problem oscillatory dipoles travelling with the body suffice to represent the vertical motion. The lift problem differs in that constant strength dipoles must be left at rest in the fluid behind the moving wing (or body). These dipoles correspond to the vortex sheet behind a moving wing. The rolling up of this vortex sheet (not considered in the linear theory used here) should introduce short wavelength internal waves which are not predicted in this report.

If a body which is stationary (except for small oscillations) exerts an oscillatory force on the stratified fluid then internal waves will radiate out from the body. If the depth of the fluid is finite there will be a maximum speed even for the longest waves. Thus one might anticipate some upstream influence for very slowly moving bodies and no upstream influence for sufficiently fast motion. Here we avoid the intermediate regime of upstream influence and study either higher speed or zero speed.

Four examples are considered here, the first three showing the effect of varying the ratio of forcing frequency to natural frequency (σ/N) with constant U/ND, and the fourth showing the result of reducing velocity (or U/ND) to zero. The last case illustrates the greatly increased amplitude of disturbances produced by confining the work input (from an oscillating force of fixed magnitude) to a local region instead of distributing it over an extended path.

In appendix F auxiliary calculations are made in a search for preferred directions.

2. Objectives and methods

Internal waves produced by a transient vertical force moving horizontally in a density-stratified fluid are considered. The aim is to develop methods for computing such waves both with and without tank walls and to present examples illustrating the tank wall effect.

Linearized time-dependent theory is used. First, a postulated solution is shown to satisfy all the boundary conditions in the presence of tank walls. But this is a 'particular integral' solution which does not satisfy the condition of zero initial disturbance. Evaluation of this solution as $t' \to -\infty$ yields a unique combination of eigenfunctions which must be subtracted from the particular integral to give a complete solution with zero initial disturbance. This procedure (replacing the use of Laplace transforms) gives the expression to be used in a tank.

The analysis in a fluid of infinite horizontal extent could be made without reference to the tank case. However it seems more economical to extend the preceding analysis. A hierarchy of large distances establishes the relative rates of oscillation of various functions which are to be integrated when the tank length and width become very large. Performing the simplified integration yields the quasi-steady state

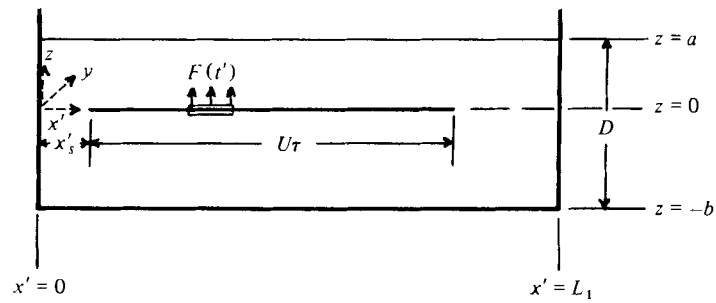

FIGURE 1. Co-ordinate system and geometry.

which applies after the body has travelled a long distance in the absence of walls. Stationary-phase approximations, if desired, can then be made in conventional fashion.

3. Development

It is assumed that the fluid is incompressible, inviscid and non-diffusive, has a constant N (Brunt–Väisälä frequency) and satisfies linearized flow equations. The fluid is confined within a rectangular tank of length L_1, width $2L_2$, and depth D. A horizontal surface of length l and width s is assumed to represent either the body planform or a small wing, depending on the dimensions chosen, but will be referred to as a wing. For simplicity the lift is considered to be uniformly distributed over the wing. The wing moves along the centre-line of the tank at an arbitrarily chosen fixed depth. It starts at a distance x'_s from the left end wall at time $t' = 0$ and travels at fixed velocity U for time τ. When the lift varies in simple harmonic fashion it is assumed to complete exactly one or three or five (etc.) cycles in the time τ.

The co-ordinates x', y, z are fixed in the fluid with origin in the left tank end wall (see figure 1). The corresponding fluid velocity components are u, v, w with subscripts U (upper) and L (lower) to indicate an imaginary division of the fluid into regions above and below the plane of the wing ($z = 0$). The free surface is then at $z = a$ and the bottom of the tank at $z = -b$, with $a + b = D$.

The natural modes of oscillation of the fluid correspond to a wavenumber $k_1 = m\pi/L_1$ in the x' direction and a wavenumber $k_2 = n\pi/L_2$ in the y direction, where m and n are integers. The resultant wavenumber is $k = (k_1^2 + k_2^2)^{\frac{1}{2}}$.

The Brunt–Väisälä frequency, N, is defined by $N^2 = -g\bar{\rho}_z/\bar{\rho}$, where g is the acceleration due to gravity, $\bar{\rho}$ is the mass density of the undisturbed fluid and the subscript z denotes differentiation. The frequency of one Fourier component of the internal wave motion (relative to co-ordinates fixed in the wing) is designated ω, and the number of cycles passed through by the simple harmonic force in time τ is n'. A parameter α is defined as

$$\alpha = [N^2(\omega + Uk_1)^{-2} - 1]^{\frac{1}{2}}. \tag{1}$$

In the regions above and below the wing the partial differential equation to be satisfied is (e.g. see Philips 1969, equation 5.2.7)

$$\nabla^2 w_{t't'} + N^2 \nabla_h^2 w = 0, \tag{2}$$

where ∇^2 is the Laplacian operator, ∇_h^2 is the two-dimensional Laplacian operator in the horizontal plane, and w is the vertical velocity of the fluid. The Boussinesq approximation has been used here.

We need a solution for w which satisfies the condition $w \cong 0$ at the free surface, $w = 0$ at the bottom, $u = 0$ at $x' = 0$ and at $x' = L_1$, and $v = 0$ at $y = \pm L_2$. Also we need at $z = 0$ to have $w_U = w_L$ and finally, with Δp the deviation from hydrostatic pressure, $\Delta p_U - \Delta p_L = 0$ except at the moving wing, where it is uniform over the wing and equal to $F(t')/sl$. $F(t')$ is the vertical force exerted by the wing on the fluid, and its maximum value is F_0.

Such a solution can be constructed by methods very similar to those used in a previous paper (Graham 1973; see also appendix A). However the reader may find it simpler if we merely postulate a solution and indicate the verification.

The following solution is suggested:

$$w_U = \frac{2F_0}{\pi\bar{\rho}sl} \sum_{-\infty}^{\infty}{}' \sum_{0}^{\infty}{}'' C_m \cos(k_1 x') A'_n k \cos(k_2 y) \times \int_{-\infty}^{\infty} \frac{\sin(\frac{1}{2}\tau\omega)\sin(k\alpha b)\sin[k\alpha(a-z)]\sin[k_1(x'_s+Ut')+\omega(t'-\frac{1}{2}\tau)]\,d\omega}{\omega\alpha(\omega+Uk_1)\sin(k\alpha D)[1-(2\pi n'/\tau\omega)^2]^*}; \quad (3)$$

the solution for w_L is the same except that $\sin(k\alpha b)\sin[k\alpha(a-z)]$ is replaced by $\sin(k\alpha a)\sin[k\alpha(b+z)]$. The bracket $[1-(2\pi n'/\tau\omega)^2]^*$ is retained only for the oscillatory force. u, v and p are found from w through the relations

$$u_{t'} = w_{zx't'}/k^2, \quad (4)$$

$$v_{t'} = w_{zyt'}/k^2, \quad (5)$$

$$\Delta p = -\bar{\rho} w_{zt'}/k^2; \quad (6)$$

and

$$C_m = \frac{1}{m\pi}\sin\left(\frac{m\pi l}{2L_1}\right), \quad A'_n = \frac{2}{n\pi}\sin\left(\frac{n\pi s}{2L_2}\right) \quad \text{with } A'_0 = \frac{s}{2L_2}. \quad (7)$$

To verify this solution we note that w varies sinusoidally with x', y, z, and t', and substitution into (2) yields (1). Setting $z = a$ or $z = -b$ gives $w = 0$ as required at the free surface and at the bottom of the tank. From (4) and (5) we obtain u and v and note that $u = 0$ at $x' = 0$ and at $x' = L_1$ while $v = 0$ at $y = \pm L_2$. At $z = 0$, w_U and w_L are both proportional to $\sin(k\alpha b)\sin(k\alpha a)$ with the same multiplying function, so continuity is satisfied between the upper and lower fluid region.

To check the lift produced by the wing we use (3) and (6) to obtain $\Delta p_U - \Delta p_L$ at $z = 0$. The terms $(x' - x'_s - Ut')$ and $(x' + x'_s + Ut')$ appear. The former is a measure of distance in co-ordinates fixed in the moving wing, and may be labelled ξ. On the other hand $(x' + x'_s + Ut')$ is a measure of distance in a co-ordinate system fixed in an image wing moving in reverse direction outside the tank. This latter term (describing the lift on the image wing) can be omitted, and we then get

$$\Delta p_U - \Delta p_L = \frac{F_0}{sl} \sum_{0}^{\infty}{}' \sum_{0}^{\infty}{}'' A_m A'_n \cos(k_1\xi)\cos(k_2 y) \times \int_0^{\infty} \frac{2\sin(\frac{1}{2}\tau\omega)\cos[\omega(t'-\frac{1}{2}\tau)]\,d\omega}{\pi\omega[1-(2\pi n'/\tau\omega)^2]^*}, \quad (8)$$

where symmetry permits the summation in m and the integration in ω to be made from 0 to ∞. The Fourier coefficients now become

$$A_m = (2/m\pi)\sin(m\pi l/2L_1) \quad \text{with} \quad A_0 = l/2L_1,$$

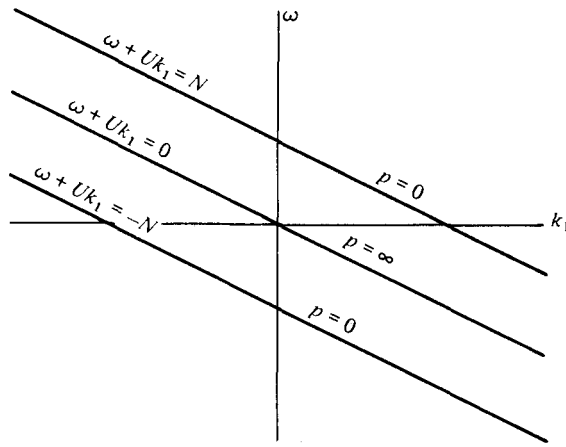

FIGURE 2. The k_1, ω plane.

and the double summation in m and n is recognizable as a double Fourier series representing 'hat' functions in ξ and y extending over the wing planform. Under the integral sign that portion of the integrand which multiplies $\cos[\omega(t'-\frac{1}{2}\tau)]$ is the Fourier transform for a 'hat' function in t' (centred on $\frac{1}{2}\tau$) if the starred bracket is omitted. If that bracket is included the transform corresponds to a sinusoidal function.

This completes the verification of the postulated equation, (3), although for further reassurance one might compute the vorticity in the fluid. (This has been done for the constant lift case but is not included here.)

It is now necessary to evaluate (3) at large negative times ($t' \to -\infty$) and remove any initial disturbance in the tank. First we go to skewed co-ordinates as shown in figure 2. Using symmetry (reflexion in the origin) the integration is performed in the half-plane above $(\omega + Uk_1) = 0$ and doubled. It then takes the form

$$w_U = \frac{4F_0}{\pi\bar{\rho}sl} \sum_{m=-\infty}^{\infty} \sum_{n=0}^{\infty} C_m A'_n \cos(k_1 x') \cos(k_2 y)\, k$$

$$\times \left\{ \int_{-Uk_1}^{N-Uk_1} \frac{\sin(k\alpha b) \sin[k\alpha(a-z)] \sin(\frac{1}{2}\tau\omega) \sin[k_1(x'_s + Ut') + (t' - \frac{1}{2}\tau)\,\omega]\, d\omega}{\omega\alpha(\omega + Uk_1) \sin(k\alpha D)\,[1-(2\pi n'/\tau\omega)^2]^*} \right.$$

$$\left. + \int_{N-Uk_1}^{\infty} \frac{\sinh(k\alpha' b) \sinh[k\alpha'(a-z)] \sin(\frac{1}{2}\tau\omega) \sin[k_1(x'_s + Ut') + (t' - \frac{1}{2}\tau)\,\omega]\, d\omega}{\omega\alpha'(\omega + Uk_1) \sinh(k\alpha' D)\,[1-(2\pi n'/\tau\omega)^2]^*} \right\}, \tag{9}$$

where
$$\alpha = [N^2(\omega + Uk_1)^{-2} - 1]^{\frac{1}{2}}$$

and
$$\alpha' = [1 - N^2(\omega + Uk_1)^{-2}]^{\frac{1}{2}}. \tag{10}$$

When t' is large and negative the final sinusoidal term in the integrand oscillates rapidly with changing ω. Such a term interacts weakly with slowly varying terms. Substantial contributions to the integral occur (*a*) when the rapidly varying function ceases to be rapidly varying (e.g. at some stationary phase points), or (*b*) when the slowly varying function becomes rapidly varying (i.e. at singular points). This case is of the latter type (see appendix B) so we look at the singular points. Such terms as ω, α, $(\omega + Uk_1)$ and $[1-(2\pi n'/\tau\omega)^2]$ appear in the denominator and may have zeros.

However there is in each case a compensating term in the numerator which prevents these zeros from creating singular points. The term $\sin(k\alpha D)$ provides all of the singular points.

For $\sin(k\alpha D) = 0$ we have

$$k\alpha D = p\pi, \tag{11}$$

where p is an integer.

Eliminating α between (10) and (11) gives

$$\omega_p + Uk_1 = N\left[1+\frac{p^2\pi^2}{k^2D^2}\right]^{-\frac{1}{2}} = f, \tag{12}$$

where ω_p is the value of ω corresponding to a particular integer p. This is the frequency of the natural mode designated by k and p (or m, n and p) as observed at the wing. f is the frequency of the same mode as seen by an observer at rest with respect to the tank.

Evaluating the contributions from the poles in (9) gives

$$w_{\mathrm{U}} = \frac{4F_0}{\bar{\rho}sl}\sum_{\substack{-\infty\\ m}}^{\infty}\sum_{\substack{0\\ n}}^{\infty} C_m A'_n \cos(k_1 x')\cos(k_2 y)$$
$$\times \sum_{\substack{0\\ p}}^{\infty} \frac{\sin(bp\pi/D)\sin[(a-z)p\pi/D]\sin[\frac{1}{2}\tau(f-Uk_1)]\cos[k_1(x'_s+\frac{1}{2}U\tau)+f(t'-\frac{1}{2}\tau)]f^2/N^2}{\cos(p\pi)\,D(f-Uk_1)[1-(2\pi n'/\tau(f-Uk_1))^2]^*}; \tag{13}$$

the expansion for w_{L} is the same except $\sin(bp\pi/D)\sin[(a-z)p\pi/D]$ becomes

$$\sin(ap\pi/D)\sin[(b+z)p\pi/D].$$

However, $b = D-a$ and p is an integer, so these two expressions are actually identical for all z and *the expression for w_{U} is valid everywhere in the tank.*

For this solution with t' large the fluid oscillates in its natural modes for the tank as a whole without regard to the interface at $z = 0$. The only discontinuity at $z = 0$ is in the parts of u and v which are independent of time. This corresponds to vorticity fixed in x, y, z co-ordinates and independent of time.

The complete solution is (9) minus (13), and for t' large and positive the solution is -2 times (13). It should be emphasized that -2 times (13) is also correct for all t' greater than τ. At $t' = \tau$ the lift force vanishes, and in this linearized inviscid theory there is then no mechanism for altering the energy in any mode or in the fixed vortex system which remains in the fluid.

3.1. *The tank with remote end walls*

We wish to make the tank very long, so that the wing can travel a long distance and the force, if oscillatory, pass through many cycles. In traversing this long path the wing should never be near the end walls, and this suggests the use of a hierarchy of large distances. We let the tank length approach infinity cubed, the path length (starting from the centre of the tank) approach infinity squared, and the far field distance approach infinity. Thus the path length is small compared to the tank length, the far field distance small compared to the path length and the wing length small compared to the far field distance.

We start with (13)† multiplied by the factor -2 which corresponds to $t' > \tau$ with no

† The subscript U on w was shown to be unnecessary and is therefore omitted.

disturbance for t' negative. A new co-ordinate, x'', is chosen to measure lengthwise distances from the centre of the tank which will be the starting point,

$$x' = x'' + \tfrac{1}{2}L_1, \quad x'_s = \tfrac{1}{2}L_1. \tag{14}$$

Then let $L_1 \to \infty^3$, multiply (13) by $-2(L_1/\pi)\,dk_1$ and integrate in k_1 from $-\infty$ to $+\infty$. Replacing $2\pi n'/\tau$ by σ, and letting $\sigma = 0$ designate the constant lift case, we get

$$\begin{aligned} w = {} & \frac{-8F_0}{\pi\bar{\rho}slD} \sum_{n=0}^{\infty} A'_n \cos(k_2 y) \sum_{p=1}^{\infty} \sin\left(\frac{bp\pi}{D}\right) \sin\left[(a-z)\frac{p\pi}{D}\right](-1)^p \\ & \times \int_{-\infty}^{\infty} \frac{f^2}{N^2 k_1} \sin(\tfrac{1}{2}k_1 l) \cos[k_1(x'' + \tfrac{1}{2}L_1)] \cos[\tfrac{1}{2}k_1 L_1 + \{\tfrac{1}{2}k_1 U\tau + f(t' - \tfrac{1}{2}\tau)\}] \\ & \times \frac{\sin[\tfrac{1}{2}(f - Uk_1)\tau]\,dk_1}{[(f - Uk_1) - \sigma^2/(f - Uk_1)]}. \end{aligned} \tag{15}$$

As L_1 becomes large $\cos^2(\frac{1}{2}k_1 L_1)$ and $\sin^2(\frac{1}{2}k_1 L_1)$ approach $\frac{1}{2}$ as an average over a small range of k_1. Similarly $\sin(\frac{1}{2}k_1 L_1)\cos(\frac{1}{2}k_1 L_1)$ approaches zero. Using these relationships, letting $t' = \tau$ and $x'' = Ut' + \xi$ and expanding trigonometric products, the integral in (15) can be expressed as the sum of two integrals:

$$\begin{aligned} & \int_{-\infty}^{\infty} \frac{f^2}{N^2} \frac{\sin(\frac{1}{2}k_1 l)}{4k_1} \frac{\sin[t'(f - Uk_1) - k_1\xi]\,dk_1}{[(f - Uk_1) - \sigma^2/(f - Uk_1)]} \\ & \qquad + \int_{-\infty}^{\infty} \frac{f^2}{N^2} \frac{\sin(\frac{1}{2}k_1 l)}{4k_1} \frac{\sin(k_1\xi)\,dk_1}{[(f - Uk_1) - \sigma^2/(f - Uk_1)]}. \end{aligned} \tag{16}$$

These two integrals can be treated separately, letting t' approach ∞^2 in the first and ξ approach ∞ in the second. The principal contributions to both integrals come in the neighbourhood of $\sigma^2 = (f - Uk_1)^2$ and have the same magnitude. However, the second one can either cancel or double the first. Defining c, f_c and k_{1c} by the following equations

$$\left.\begin{aligned} c &= (\partial f/\partial k_1)_{k_{1c}} - U, \quad f_c = \pm\sigma + Uk_{1c}, \\ k_{1c} &= \frac{N}{U}\left[1 + \frac{p^2\pi^2}{(k_{1c}^2 + k_2^2)D^2}\right]^{-\frac{1}{2}} \mp \frac{\sigma}{U}, \end{aligned}\right\} \tag{17}$$

the vertical velocity produced by the internal wave system becomes

$$\begin{aligned} w = {} & \frac{-F_0}{\bar{\rho}slD} \sum_{n=0}^{\infty} A'_n \cos(k_2 y) \sum_{p=1}^{\infty} (-1)^p \sin(bp\pi/D) \sin[(a-z)\,p\pi/D] \\ & \times \frac{f_c^2}{N^2} \frac{\sin(\frac{1}{2}k_{1c} l)\cos(k_{1c}\xi)}{k_{1c}|c|} \left[1 + \frac{|c|}{c}\frac{\xi}{|\xi|}\right] \end{aligned} \tag{18}$$

and twice this for $\sigma = 0$.

Here the tank length, L_1, approaches ∞^3, the distance travelled by the wing, Ut', approaches ∞^2 and the far field distance, $|\xi|$, approaches ∞. k_{1c} is defined implicitly in the last equation of (17), but solutions are readily obtainable by iteration for many problems.

3.2. *The tank with remote end and side walls*

Let L_2, the half-width of the tank, approach ∞^3. To change from a summation to an integration we multiply (18) by $(L_2/\pi)\,dk_2$. The integrand then contains $(\partial f/\partial k_1)_{k_{1c}} - U$, which is c. This is a function of k_2, the variable of integration. To simplify the analysis we discard those cases in which c passes through zero within the range of integration.

It is shown in appendix C that $U > ND/\pi$ is a sufficient condition for the exclusion of such cases.† This is a particularly convenient condition to impose since it also ensures that there are not more than two values of k_{1c} to consider (i.e. the last equation of (17) has a single root when the sign choice has been made). Also, as indicated in appendix C, a convergent iteration process is available for determining k_{1c}.

With the above restriction, $U > ND/\pi$, the term $[1+|c|\,\xi/c\,|\xi|]$ can be taken outside the integral sign, and $[(\partial f/\partial k_1)_{k_{1c}} - U]^{-1}$ is not singular.

Ahead of the wing the term $[1+|c|\,\xi/c\,|\xi|]$ becomes zero, and behind the wing it takes on the value two, so that behind the wing w becomes

$$w = \frac{-4F_0}{\pi\bar{\rho}slD} \sum_{\substack{1\\p}}^{\infty} (-1)^p \sin\left(\frac{bp\pi}{D}\right) \sin\left[(a-z)\frac{p\pi}{D}\right] \times \int_0^{\infty} \frac{\sin(\frac{1}{2}k_2 s)}{k_2} \frac{f_c^2}{N^2} \frac{\sin(\frac{1}{2}k_{1c} l)\cos(k_2 y)\cos(k_{1c}\xi)\,dk_2}{k_{1c}|(\partial f/\partial k_1)_{k_{1c}} - U|} \tag{19}$$

and twice this for $\sigma = 0$, where only one value of k_{1c} exists. For $\sigma \neq 0$ there are two values of k_{1c} whose contributions to w must be added. U/ND must be greater than $1/\pi$.

3.3. *Stationary phase analysis with y large*

Let y as well as ξ approach ∞ and $\cos(k_2 y)\cos(k_{1c}\xi)$ in (19) becomes the rapidly oscillating part of the integrand as k_2 varies. The vertical velocity produced by the internal wave system at the completion of an odd number of cycles is then, by stationary phase analysis,

$$w = \frac{-2F_0(2/\pi)^{\frac{1}{2}}}{\bar{\rho}slD} \sum_{\substack{1\\p}}^{\infty} (-1)^p \sin\left(\frac{bp\pi}{D}\right) \sin\left[(a-z)\frac{p\pi}{D}\right] \times \frac{f_{cc}^2}{N^2} \frac{\sin(\frac{1}{2}k_{2c} s)}{k_{2c}} \frac{\sin(\frac{1}{2}k_{1cc} l)\,\mathrm{tg}\,(\gamma_c + \frac{1}{4}\pi)}{k_{1cc}|(\partial f/\partial k_1)_{k_{1cc}} - U| \times |(\partial^2 k_{1c}/\partial k_2^2)_{k_{2c}}\,\xi|^{\frac{1}{2}}}, \tag{20}$$

and twice this for $\sigma = 0$, where

$$\mathrm{tg}(x) = \sin x \quad \text{if } \xi(\partial^2 k_{1c}/\partial k_2^2)_{k_{2c}} \text{ is negative,}$$
$$\mathrm{tg}(x) = \cos x \quad \text{if } \xi(\partial^2 k_{1c}/\partial k_2^2)_{k_{2c}} \text{ is positive.}$$

Here $\gamma_c = (k_{2c} y + k_{1cc}\xi)$, ξ is negative, y is positive and $U > ND/\pi$. The quantity k_{2c} is defined by $\partial\gamma/\partial k_2 = 0$ and k_{1cc} is k_{1c} evaluated at $k_2 = k_{2c}$.

3.4. *Stationary phase analysis for U = 0*

When the wing is stationary the distance travelled, Ut', can no longer be the intermediate distance in the hierarchy of large distances previously used. Instead the velocity $(\partial f/\partial k_1)_{k_{1c}}$ (related to the group velocity) replaces U, and multiplied by t' must be much less than the tank dimensions and much greater than the distance out from the wing to the observation point.

With U set equal to zero (19) can be used for the stationary phase analysis. The vertical velocity then becomes

$$w = \frac{-2\sqrt{(2/\pi)}\,F_0}{\bar{\rho}slD} \sum_{\substack{1\\p}}^{\infty} \sin\left(\frac{bp\pi}{D}\right) \sin\left[(a-z)\frac{p\pi}{D}\right] \frac{\sigma}{N^2-\sigma^2} \times \frac{\sin(\frac{1}{2}Ps\sin\theta)\sin(\frac{1}{2}Pl\cos\theta)}{\sin\theta\cos\theta} \frac{\cos(Pr - \frac{1}{4}\pi)}{(Pr)^{\frac{1}{2}}}, \tag{21}$$

† If $\sigma/N > 1 + 2/3\sqrt{3}$ the condition becomes merely $U > 0$.

where $P = p\pi\sigma/D(N^2-\sigma^2)^{\frac{1}{2}}$, and y and ξ have been replaced by $r\sin\theta$ and $r\cos\theta$, respectively.

This result applies for $\sigma < N$. There is no real k_{1c} and no stationary phase contribution when the forcing frequency exceeds the Brunt–Väisälä frequency. This was pointed out by Mowbray & Rarity (1967) in a two-dimensional study.

This result applies at distances out from the wing which are large compared to the wing dimensions and at the completion of a large number of cycles. The lift oscillations on the wing must have continued for a time t' which is much greater than

$$p\pi r/[DN(1-\sigma^2/N^2)^{\frac{3}{2}}],$$

where r is the radius to the observation point.

It is interesting to note from the term $\cos(Pr-\frac{1}{4}\pi)$ that the disturbance pattern tends to repeat (with modified amplitude) at intervals in r such that

$$\Delta r = (2D/\sigma)(N^2-\sigma^2)^{\frac{1}{2}}.$$

The contribution from each value of p is scaled down in the same proportion,

$$[r/(r+\Delta r)]^{\frac{1}{2}}.$$

The ratio of the horizontal interval Δr to the depth D ($\Delta r/D = 2(N^2-\sigma^2)^{\frac{1}{2}}/\sigma$) suggests reflected waves with a preferred angle of propagation in a vertical plane. Preferred directions are discussed by Mowbray & Rarity (1967) in connexion with a two-dimensional problem, and by Hendershott (1969) for a three-dimensional example.

4. Examples

4.1. *Calculation methods*

Equation (13) multiplied by -2, and equations (18), (19), (20) and (21) can be used to calculate the vertical velocity produced by the internal waves.† In all cases the depth, D, is finite. Equation (13) applies to a rectangular tank with both end walls and side walls. A triple summation is required, which may be time-consuming, but the results are valid everywhere in the tank. In (18) the end walls are removed, the oscillating force is assumed to have operated for a long time and the observation point must be far behind the wing. Only a double summation (in n and p) is required. Equation (19) is obtained by removing both end walls and side walls. Integration in k_2 replaces summation over n, and near the path (i.e. where y is small) the integration is readily performed. In (20), a stationary phase analysis, both the lateral and longitudinal distance to the observation point must be large. In the particular examples chosen here (20) is less useful than (19). Equation (21) applies to a stationary wing and the stationary phase analysis requires that observations be made in the far field long after the initial application of the oscillatory force.

Convergence of the summations presents some problems. Figure 3 shows a typical example for a double summation in p and n. With $m = 2$ and n summed from zero to eighty we examine the effect of summing p to various limits, $\bar{p}$. The ordinate of the curve is the summation

$$W = -\sum_{p=1}^{\bar{p}}\sum_{n=0}^{80}\frac{w_z\bar{\rho}slD^2N}{2\pi F_0}\times 10^4 \tag{22}$$

† Only (13), (19) and (21) are used in the primary calculations of this paper.

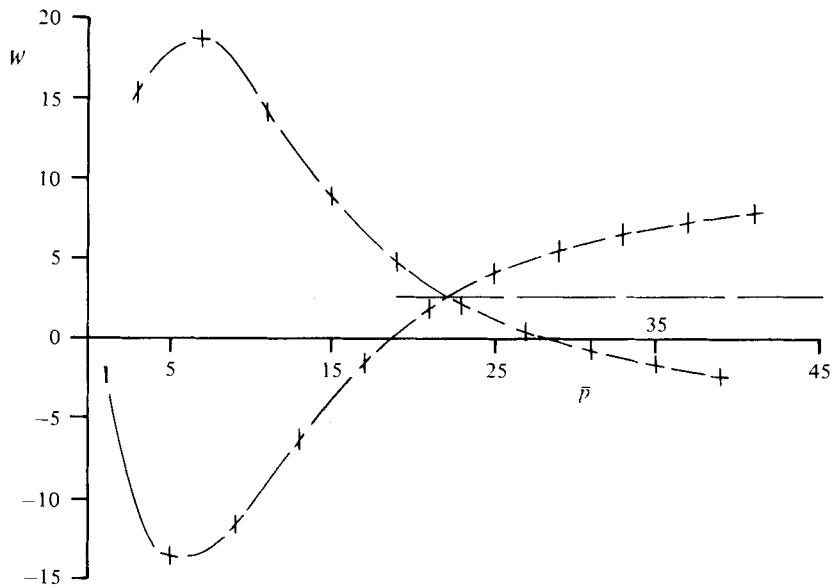

FIGURE 3. Convergence of a double summation. $m = 2$,

$$W = -\sum_{p=1}^{\bar{p}} \sum_{n=0}^{80} \frac{w_z \bar{\rho} s l D^2 N}{2\pi F_0} \times 10^4.$$

and the abscissa is $\bar{p}$, which in this case takes on only odd integral values. For $\bar{p} = 1$ $W = -2{\cdot}39$, for $\bar{p} = 3$ $W = +15{\cdot}25$, for $\bar{p} = 5$ $W = -13{\cdot}56$, etc. This oscillation continues until the envelope curves cross (between 21 and 23 on the $\bar{p}$ scale). Then a smaller amplitude oscillation begins, suggesting ultimate convergence at $W \cong 2{\cdot}6$. However it would be necessary to extend $\bar{p}$ to a much higher value to verify this.

Because of the difficulty just described it is desirable to improve convergence by considering that the lift on the wing is distributed vertically over a small distance 2ϵ. Also we find w at a distance ϵ below the free surface (see appendix D). Dividing this w by ϵ then gives an average strain rate in a surface layer of thickness ϵ. In a 'typical' case an ϵ/D of 0·04 increases $w(a-\epsilon)/\epsilon$ by approximately three per cent over the value for $\epsilon/D = 0$. Such averaging broadens and lowers very sharp peaks but does not eliminate them. The effect on relatively smooth velocity profiles is slight since averaging affects primarily the 'fine structure' (short wavelengths) of the flow pattern.

Having improved the convergence in p it is then desirable (as shown by experience) to sum first and most extensively in p, terminating the series where $p\epsilon/D$ is an integer. In practice this tends to eliminate spurious contributions both from higher n (or k_2) terms and from the higher p values. Extension of the n (or k_2) range alone often introduces terms which do not appear to converge satisfactorily. However, an adequate extension of the p limit generally shows that the contributions from n (or k_2) extension are negligible.

In addition to the vertical averaging described (which results in the calculation of $w(a-\epsilon)/\epsilon$) other minor changes are made in (13) etc. before computation. Instead of k_1 and k_2 the non-dimensional K_1 and K_2 are used, with $K_1 = k_1 D$, etc. Also, certain parameters and constants are transferred to the left-hand side and form a dimensionless variable with w (see appendix E).

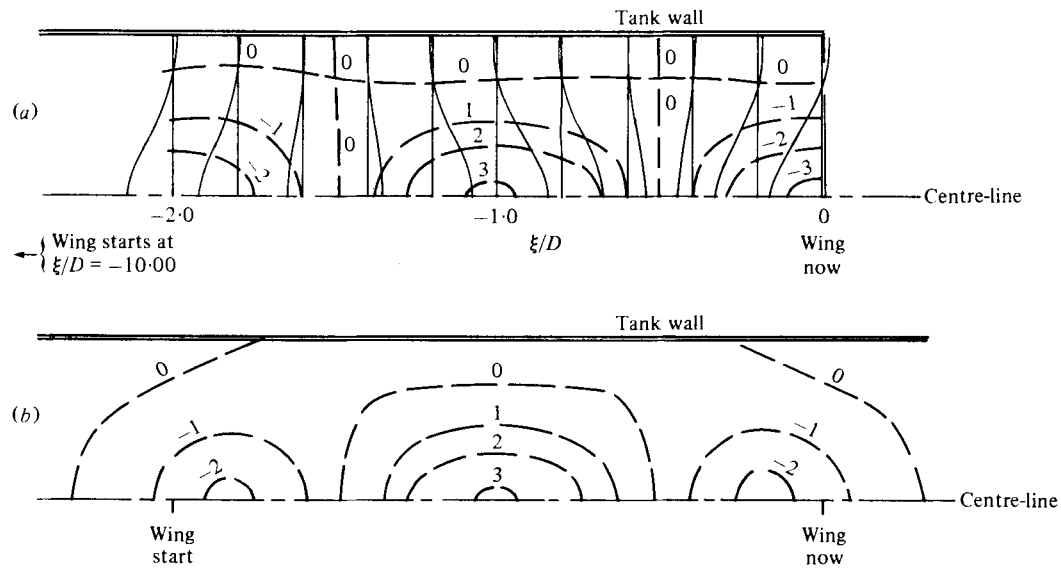

FIGURE 4. Contours of constant $\tilde{w}(a-\epsilon)/\epsilon$ for $\sigma/N = 5\pi$, example 1. (*a*) $n' = 5$, $L_1/D = 10$. (*b*) $n' = 1$, $L_1/D = 6$.

4.2. *Discussion of examples*

In all examples the wing is in a plane halfway between the free surface and the bottom. The wing exerts a vertical force on the fluid which starts at time zero, drops to zero at a certain time τ and remains zero thereafter. The time τ is also the time for observing the vertical velocity w, and, in the case of the oscillatory force, corresponds to the completion of an odd integral number of cycles. The distance ϵ is defined by $\epsilon/D = 0{\cdot}04$ in all cases. The quantity $(-w(a-\epsilon)\bar{\rho}slD^2N/\epsilon 2\pi F_0) \times 10^4$, labelled $\tilde{w}(a-\epsilon)/\epsilon$, is calculated for all cases. The average strain rate is $w(a-\epsilon)/\epsilon$. The average

$$dw/dz = -w(a-\epsilon)/\epsilon.$$

Example 1. In the first example the oscillatory force has a frequency 5π times the natural frequency ($\sigma/N = 5\pi$). The tank length is varied from two to six to ten times the depth ($L_1/D = 2$, 6, or 10). The width equals the depth ($2L_2/D = 1$). The rectangular planform wing measures two and one-half percent of the depth in the direction of motion and seven and one-half per cent laterally ($l/D = 0{\cdot}025$, $s/D = 0{\cdot}075$). The velocity of the wing is five times the product of total depth and Brunt–Väisälä frequency ($U/ND = 5$, Froude number $= 2\pi U/ND = 10\pi$).

Figure 4(*a*) shows contours of constant $\tilde{w}(a-\epsilon)/\epsilon$ for the case where $L_1/D = 10$. These contours are shown for the cycle immediately behind the wing. The cases where $L_1/D = 6$ and 2 are not separately shown because the contours are identical with $L_1/D = 10$ within the accuracy of plotting. Figure 4(*b*) shows similar data for a case in which $L_1/D = 6$ and the wing starts one-third of the tank length from the left end wall, travelling over the middle third of the tank only. The contours strongly resemble those in figure 4(*a*), but the start and end of the pattern show appreciable effects from the change of boundary conditions at the ends of this single cycle. The absence of the

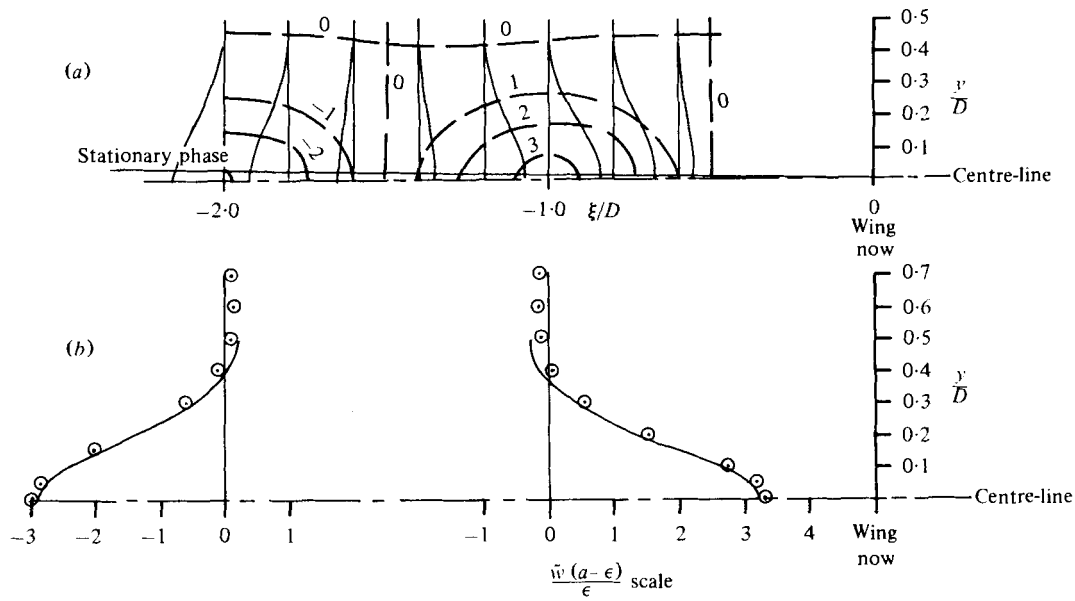

FIGURE 5. Comparison of $\tilde{w}(a-\epsilon)/\epsilon$ for tank and no-wall cases, $\sigma/N = 5\pi$, example 1. (*a*) No walls, $n' \to \infty$. (*b*) ○, no walls, $n' \to \infty$; ——, tank, $L_1/D = 10$, $L_2/D = 0{\cdot}5$, $n' = 5$.

end wall at completion of the cycle and the lack of a continued pattern at the beginning of the cycle appear to have similar effects.

The rapid establishment of the typical pattern is somewhat surprising. Calculations were also made with the walls removed and after many cycles had been completed (see figure 5*a*). The agreement with calculations for the tank (see figure 5*b*) is evident. Note that the no-wall analysis uses (19) modified for computation, and is not a stationary phase analysis. The latter would show zero disturbance outside the very narrow wedge indicated in figure 5(*a*).

Example 2. The frequency of the oscillatory force is reduced to four times the natural frequency here ($\sigma/N = 4$). The wing velocity is the same as before ($U/ND = 5$, Froude number $= 10\pi$). The tank width is the same as before ($L_2/D = 0{\cdot}5$), and the wing planform is unchanged.

The tank is first made just long enough to accommodate one cycle ($L_1/D = 2{\cdot}5\pi$), then long enough for three cycles ($L_1/D = 7{\cdot}5\pi$). The values of $\tilde{w}(a-\epsilon)/\epsilon$ are almost identical in the cycle immediately behind the wing. These results are shown as one curve in figure 6(*b*), labelled $L_2/D = 0{\cdot}5$. Calculations were also made after many cycles with all walls removed and these results are significantly different (see figure 6*b*). The tank width was then doubled ($L_2/D = 1{\cdot}0$), and these results (in figure 6*a* and *b*) show generally good agreement with the calculations for many cycles with walls removed. Only in the vicinity of the sidewall are the differences appreciable, which might be expected. This suggests that the pattern is quickly established but agrees with the no-wall case only if the tank width is sufficiently large.

Stationary phase analysis would show all disturbances confined to the narrow wedge indicated in figure 6(*a*).

Example 3. The wing carries a constant lift in this case ($\sigma/N = 0$). The wing planform

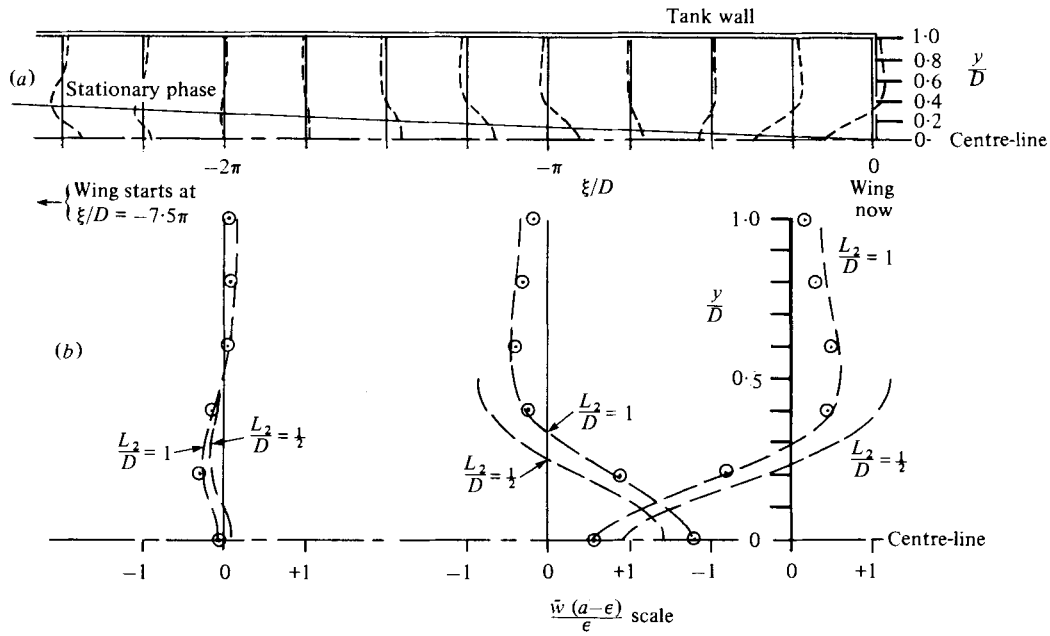

FIGURE 6. Comparison of $\tilde{w}(a-\epsilon)/\epsilon$ for tank and no-wall cases, $\sigma/N = 4$, example 2. (*a*) $n' = 3$, $L_1/D = 7{\cdot}5\pi$. (*b*) ⊙, no walls, $n' \to \infty$.

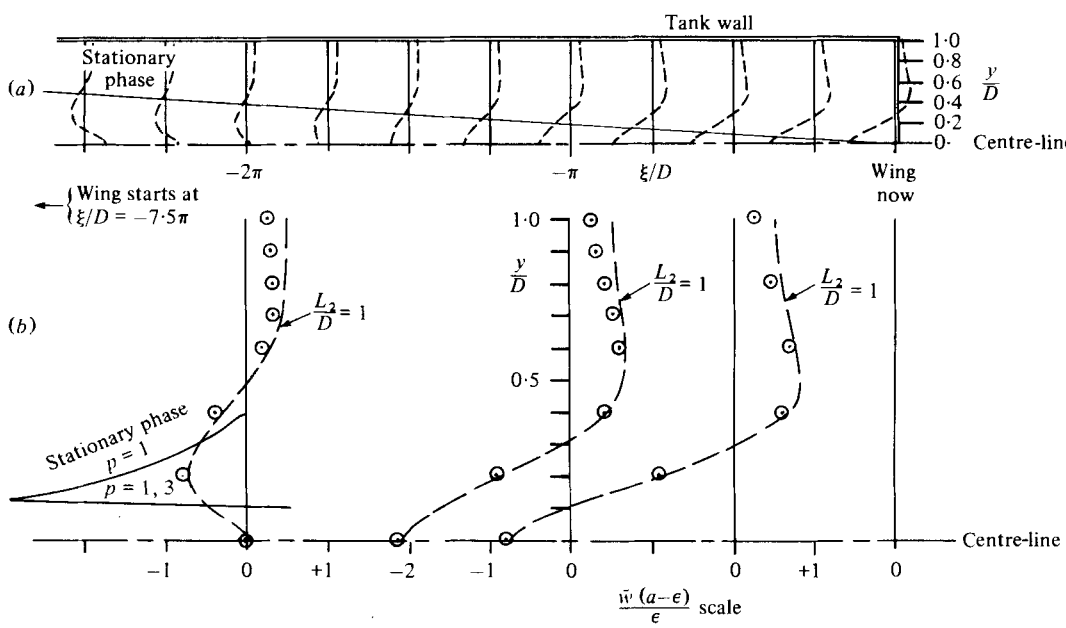

FIGURE 7. Comparison of $\tilde{w}(a-\epsilon)/\epsilon$ for tank and no-wall cases, constant lift, example 3. (*a*) $L_1/D = 7{\cdot}5\pi$. (*b*) ⊙, no walls, $\tau \to \infty$.

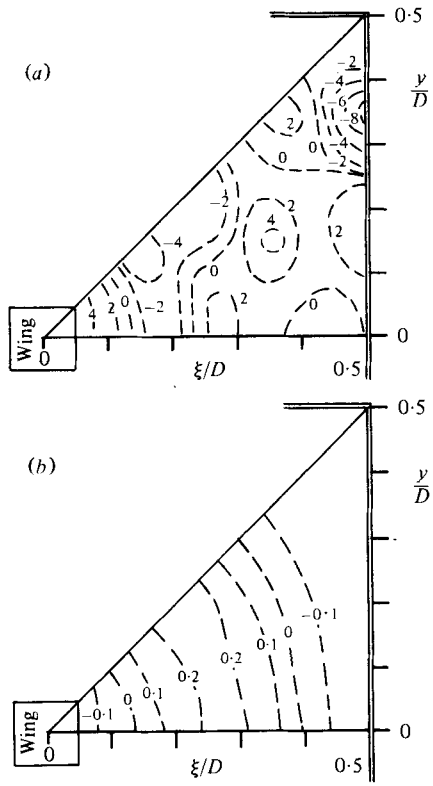

FIGURE 8. Contours of constant $\tilde{w}(a-\epsilon)/\epsilon$ for stationary wing, $\sigma/N = \frac{1}{2}$, example 4. (*a*) $n' = 5$. (*b*) $n' = 1$. $\tilde{w}(a-\epsilon)/\epsilon$ = contour label $\times 10^4$.

and wing velocity ($U/ND = 5$) are unchanged, and the tank width is the same as in the last part of example 2 ($L_2/D = 1{\cdot}0$).

Figure 7 (*a*) shows lateral profiles of $\tilde{w}(a-\epsilon)/\epsilon$ at ten streamwise stations in the tank extending downstream from the wing (at the right-hand tank end-wall) for a distance defined by $\xi/D = 2{\cdot}5\pi$, the total length of the tank corresponding to $7{\cdot}5\pi$. Below, figure 7 (*b*), are shown in expanded co-ordinates the $\tilde{w}(a-\epsilon)/\epsilon$ values for three typical stations. The values in the tank are labelled $L_2/D = 1{\cdot}0$. A no-wall calculation indicated by points is included for comparison. As in the preceding example the agreement is good near the wing path and the introduction of the wall appears to exaggerate disturbances only in the wall neighbourhood.

Typical stationary phase results are shown in figure 7 (*b*). They are confined to the wedge appearing in figure 7 (*a*), and would become useful much further downstream.

Example 4. We now set $U/ND = 0$, and for simplicity make the wing planform square ($l/D = s/D = 0{\cdot}1$), and the tank square ($L_1/D = 2L_2/D = 1{\cdot}0$). The wing is placed at the centre of the tank ($x_s'/D = 0{\cdot}5$) and exerts an oscillatory force on the fluid with frequency equal to half the natural frequency ($\sigma/N = 0{\cdot}5$).

For a wing force stopping after one cycle the contours of constant $\tilde{w}(a-\epsilon)/\epsilon$ are given in figure 8 (*b*). Because of the symmetry only one octant is shown and this indicates a basically circular wave pattern. When the wing force goes through three cycles and stops, the quasi-circular pattern is confined to the inner half 'radius' of the tank,

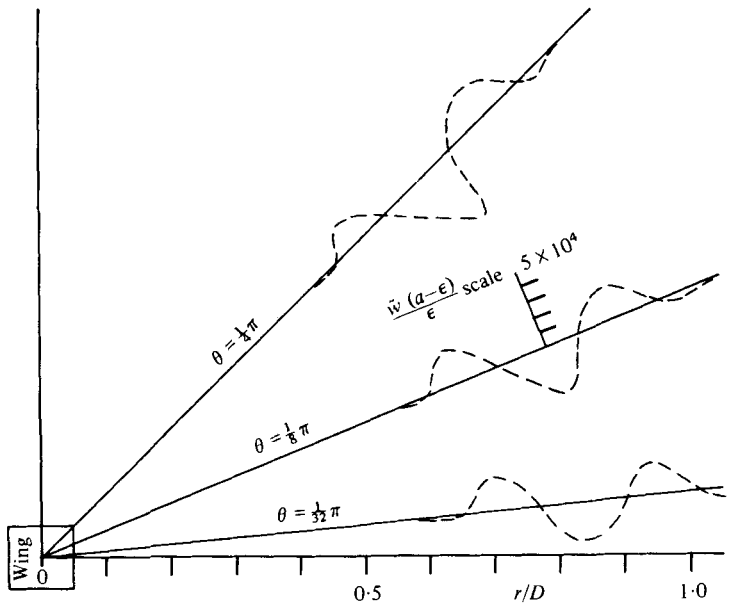

FIGURE 9. $\tilde{w}(a-\epsilon)/\epsilon$ for a stationary wing, no walls, $\sigma/N = \frac{1}{2}$, $\tau \to \infty$, example 4.

and the outer portion is apparently altered by reflected waves (case not shown here). In figure 8(*a*) the pattern produced by five cycles of force appears. Here the reflected waves have apparently had time to erode most of the basically circular pattern except for the inner quarter of the tank 'radius'. The amplitude of the disturbances is now approximately twenty times that for the one-cycle case.

Also of interest is the large increase in amplitude (by factors of 10^3 and 10^4) over the moving wing cases. This is probably caused by the continuous feeding of energy into a small volume of fluid for the stationary wing.

In figure 9 we show radial profiles of $\tilde{w}(a-\epsilon)/\epsilon$ for a no-wall case after many cycles of operation. For the first time in this paper a stationary phase analysis is convenient for obtaining no-wall results. The radial profiles at three different angles are quite similar, emphasizing the basically circular pattern. Disturbances are nearly zero outside the r/D range 0·65 to 1·10 in figure 9, but regions of large disturbance are periodically repeated at intervals $(N^2-\sigma^2)^{\frac{1}{2}}(2/\sigma)$ in r/D as mentioned in the discussion of (21). This corresponds to waves reflected alternately from the top and bottom of the fluid with a preferred direction of 30° to the horizontal. This angle is in agreement with that shown by Mowbray & Rarity (1967) and by Hendershott (1969).

The magnitudes shown in figure 9 are about half those for the five-cycle case in the tank (figure 8*a*). This is probably an indication of the energy which escapes into the surrounding fluid when no walls are present.

5. Discussion of results

5.1. *Comparison of tank and no-wall results*

generally good for the moving-wing cases. The exception is example 2 ($\sigma/N = 4$) when For the examples chosen the agreement between tank and no-wall flow patterns is

the tank width equals the depth ($L_2/D = \frac{1}{2}$). Increasing the tank width to twice the depth ($L_2/D = 1$) produces good agreement for that case. In all cases, as one would expect, the two solutions being compared differ near the tank walls. For all the moving wing cases $U/ND = 5$, and other values of this parameter as well as other wing geometries and locations require investigation before general statements can be made about the significance of tank wall effects.

The stationary wing case shows poor agreement. It might perhaps be anticipated that with protracted feeding of energy into a localized fluid region any quasi-steady state approached could be seriously altered by removing the walls and allowing energy to escape.

5.2. *Repetition of the wave pattern*

The quick establishment of the wave pattern and its repetition are especially noticeable for example 1, figures 4 and 5. From (19) or (E 3) we see that behind the wing the fluctuation of $\tilde{w}(a-\epsilon)/\epsilon$ with ξ (distance in the direction of motion) depends only on $\cos(K_{1c}\xi/D)$. In the special case when U/ND and σ/N approach infinity

$$K_{1c} \cong \mp \sigma D/U$$

if ξ/D is fixed. Then the $\cos(K_{1c}\xi/D)$ can be removed from under the integration and summation signs and the flow pattern repeats in ξ with period $2\pi U/\sigma$. Example 1 with $U/ND = 5$ and $\sigma/N = 5\pi$ approximates this condition.

5.3. *Preferred directions*

Disturbances in the flow are in general largest near the wing and decrease with increasing distance from the wing. In certain 'preferred' directions the rate of amplitude decrease with increasing distance is less than for non-preferred directions. Stationary phase analysis yields these preferred directions which, for our finite depth analysis, would be vertical planes through the wing inclined outward to the wing track. Far behind the regions of largest disturbance which we have studied, stationary phase methods would apply and such preferred directions would appear for examples 1 and 2.

Rehm & Radt (1975) assumed *infinite* depth and, applying stationary phase methods in three dimensions, found preferred directions (rays from the body) inclined both laterally and to the horizontal. For such an analysis to apply with finite depth the observation point should be both close to the body in terms of depth and far from the body in terms of wavelengths. In examples 1 and 2 the typical wavelengths ($2\pi D/K_{1c}$) are greater than the depth so three-dimensional stationary phase results cannot exist.

Appendix F illustrates this point. First, a survey of w is made in a vertical plane behind the wing and normal to the wing path using the parameters of example 2. Figure 10 shows this and the dominant feature is the high velocities induced by trailing vortex lines left in the fluid. This is a feature which does not appear in the heaving problem studied by Rehm & Radt, and might tend to obscure preferred directions. To see other features of the velocity field we remove the trailing vortices by making the wing span very large ($s/D \to \infty$). Figure 11 shows a survey of w along a vertical line behind the wing for $\sigma/N = 4$ and three values of U/ND. Only for values of U/ND much lower than 5 (used in examples 1 and 2) are preferred directions apparent. The

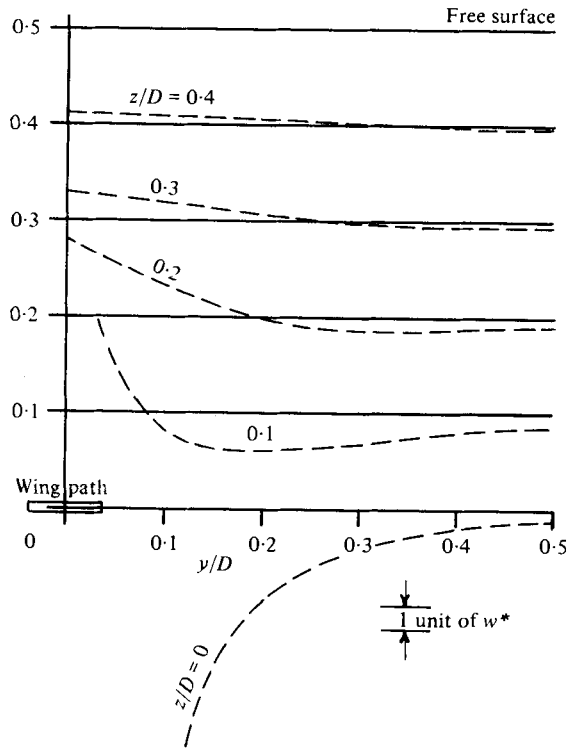

FIGURE 10. Survey of w^* in a vertical plane,

$$w^* = \frac{w\pi\bar{\rho}slDN \times 10^4}{4F_0}, \quad \sigma/N = 4{\cdot}0, \quad U/ND = 5, \quad \xi/D = -\tfrac{1}{2}\pi, \quad \text{no wall.}$$

inclination to the horizontal is approximately in agreement with the results of Rehm & Radt (roughly 2 to 6 degrees).

For example 4, the stationary wing, preferred directions appear and are in agreement with the results of Mowbray & Rarity and of Hendershott.

Appendix A. Description of method of obtaining equation (3)

A wing of rectangular planform is to start at a given time and place, move through the fluid horizontally at constant speed, then stop at a prescribed time. While the wing moves on this path it supports a pressure difference between the under side and the upper side (the same at all points on the wing). The vertical force or lift so carried may be constant or vary in simple harmonic fashion during the time the wing moves, but must in either case be zero at all other times.

We first divide the fluid by passing an imaginary horizontal plane through the fluid at the level of the wing and consider separately solutions of the partial differential equation in the upper and lower regions. These solutions, periodic in both space and time, are chosen so that vertical velocity is continuous across the plane but pressure is discontinuous. They are also chosen to represent standing waves in a co-ordinate system fixed in the moving wing. Thus in the wing co-ordinate system we have a set of

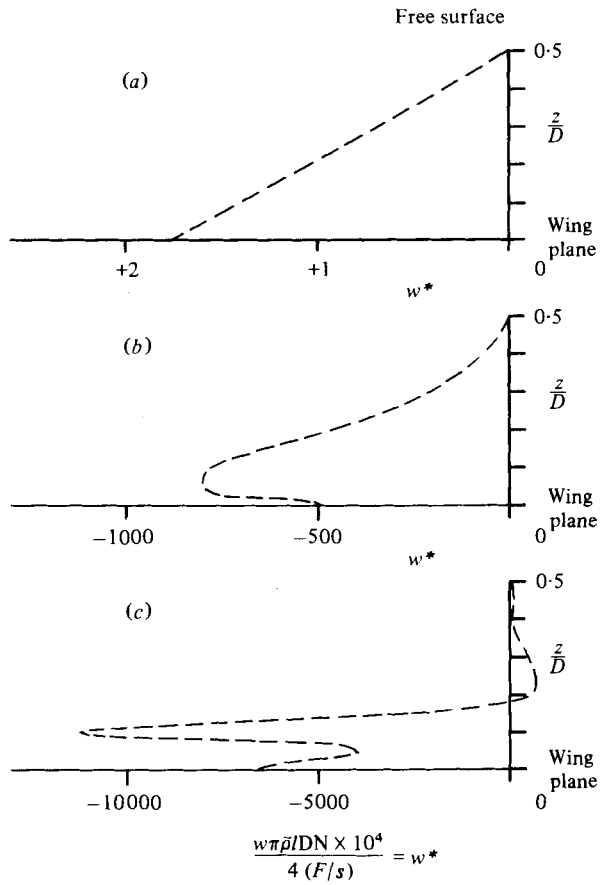

FIGURE 11. Preferred directions, $s/D \to \infty$, $\xi/D = -\frac{1}{2}\pi$, $\sigma/N = 4$, $\epsilon/D = 0$. (*a*) $U/ND = 5{\cdot}0$. (*b*) $U/ND = 0{\cdot}5$. (*c*) $U/ND = 0{\cdot}1$.

discrete wavelengths of spatially periodic lift distributions extending over the entire plane separating upper and lower fluid. These periodic distributions in space have fixed nodes, but may fluctuate in time with a continuous spectrum of frequencies, ω. The problem is first to combine the spatial distributions in a double Fourier series to represent the lift confined to the wing planform (and images).

Then the continuous spectrum of frequencies must be utilized (in a Fourier integral) to represent the desired time history of the lift, which is zero until the wing starts moving, then constant (or varying sinusoidally) until the wing stops, then zero from that time on.

Solutions for the upper fluid must satisfy the boundary condition $w \cong 0$ at the free surface. Solutions for the lower region must satisfy a similar condition, $w = 0$, at the bottom. The Fourier series representation laterally produces an infinite set of images laterally and permits the insertion of tank side walls in vertical planes of symmetry. To obtain planes of symmetry in which the end walls can be inserted is a little more difficult, since the wing changes its distance from the end walls. This can be accomplished by superimposing on the forward-moving system (the wing with doubly infinite set of images) a similar system moving in the opposite direction. Then halfway

between a forward-moving wing and a backward-moving wing (or image) there is a plane of symmetry at rest with respect to the fluid. In such a plane an end wall can be inserted.

By such methods the proposed equation for w, (3), was obtained.

Appendix B. Discussion of absence of stationary phase points in equation (9)

When ω approaches $-Uk_1$ or $N-Uk_1$ in the first integral of (9) $d\alpha/d\omega$ approaches ∞. The terms $\sin(k\alpha b)$, $\sin[k\alpha(a-z)]$ in the numerator and $\sin(k\alpha D)$ in the denominator then oscillate rapidly with small changes in ω. It might appear that stationary-phase points could be defined by suitably combining terms in the numerator. However the rapidly oscillating term in the denominator does not fit into this picture.

More generally one can perhaps reason as follows. The first integral in (9) can be rewritten as

$$\lim_{\epsilon\to 0}\int_{-Uk_1+\epsilon}^{N-Uk_1-\epsilon}\ldots d\omega.$$

For each ϵ a lower bound can be set on $|t'|$ such that $|t'|$ is always much greater than terms such as $d(k\alpha b)/d\omega$. It is then possible for ϵ to approach zero and $|t'|$ to approach infinity in such a fashion that stationary-phase points never appear within (or on the boundaries of) the region of integration. This applies in the limit $\epsilon\to 0$ since, although $|t'|$ and $d(k\alpha b)/d\omega$ both become infinite, $|t'|$ is, nevertheless, much greater throughout the closed region of integration.

Appendix C. The condition $U/ND > 1/\pi$†

This condition is sufficient to ensure that $(\partial f/\partial k_1)_{k_{1c}}$ is always less than U, that the equation defining k_{1c} has only one real root for each sign choice, and that a simple iteration process converges for these roots.

(*a*) *Derivation of lower bound*

It is required that $(\partial f/\partial k_1)_{k_{1c}}$ be always less than U or, with $K_1 = k_1 D$ and $K_2 = k_2 D$, that $(\partial[f/N]/\partial K_1)_{K_{1c}}$ be always less than U/ND. This is to ensure that

$$[(\partial(f/N)/\partial K_1)_{K_{1c}} - U/ND]$$

does not pass through zero as K_2 varies from zero to infinity. Differentiating (12) and using K_{1c} and K_2 instead of k_{1c} and k_2, we get

$$U/ND > \left\{\frac{p^2\pi^2 K_{1c}}{(K_{1c}^2+K_2^2+p^2\pi^2)^{\frac{3}{2}}(K_{1c}^2+K_2^2)^{\frac{1}{2}}}\right\}. \tag{C 1}$$

To get a lower bound on U/ND we need an upper bound on the right-hand side. If we assume K_{1c} and K_2 independent and let them take on all possible positive values, then the greatest value for the bracket in (C 1) occurs when $K_2 = 0$ regardless of K_{1c} and p. The resulting inequality is

$$U/ND > [p^2\pi^2/(K_{1c}^2+p^2\pi^2)^{\frac{3}{2}}]. \tag{C 2}$$

† Note that stationary phase restrictions are not used here.

The greatest value of the [ ] occurs when $K_{1c} = 0$ regardless of the value of p. For $K_{1c} = 0$,

$$U/ND > (1/p\pi). \tag{C 3}$$

The greatest value of the ( ) occurs when $p = 1$. The lower bound on U/ND is then $1/\pi$ and the restriction

$$U/ND > 1/\pi \tag{C 4}$$

prevents $[(\partial(f/N)/\partial K_1)_{K_{1c}} - U/ND]$ from passing through zero in the integration range of K_2.

(*b*) *Roots of the equation defining* K_{1c}

The last equation of (17) is rewritten with k_1 instead of k_{1c} and $K_1 = k_1 D$ to give

$$K_1 = \left[\left(1 + \frac{p^2\pi^2}{K_1^2 + K_2^2}\right)^{-\frac{1}{2}} \mp \frac{\sigma}{N}\right] \frac{ND}{U}. \tag{C 5}$$

The roots of the equation are obtained by plotting the left-hand side and the right-hand side against K_1 and noting the intersections. Fix the sign preceding σ/N, and note that only one intersection is possible if the slope of the right-hand side is less than unity. The right-hand side is $(f/N).(ND/U)$ plus a constant, and its slope is

$$(\partial(f/N)/\partial K_1).(ND/U).$$

The condition is then

$$\partial(f/N)/\partial K_1 < U/ND. \tag{C 6}$$

However, this is the same restriction as that considered in (*a*), and a sufficient condition for compliance is

$$U/ND > 1/\pi. \tag{C 7}$$

(*c*) *Convergence of the iteration process for* K_{1c}

The left-hand side of (C 5) plotted against K_1 is a straight line through the origin with unit slope. The right-hand side has a lesser magnitude of slope if $(U/ND) > 1/\pi$ as shown above. The iteration process consists of assuming a trial K_1, substituting this in the right-hand side and solving for the left-hand side. This new K_1 is substituted in the right-hand side and a new left-hand side is found, etc. It can be shown graphically that this process converges when the absolute magnitude of the slope on the right-hand side is less than that on the left-hand side (i.e. less than unity).

If the forcing frequency is greater than the natural frequency ($\sigma/N > 1$) the restriction $U/ND > 1/\pi$ which applies in (*a*), (*b*) and (*c*) above may be relaxed. In that case we get from (C 5) that

$$K_{1c}^2 > (ND/U)^2(\sigma/N - 1)^2 \tag{C 8}$$

and (C 2) becomes

$$\left(\frac{U}{ND}\right) > \frac{p^2\pi^2}{[(ND/U)^2(\sigma/N - 1)^2 + p^2\pi^2]^{\frac{1}{2}}}. \tag{C 9}$$

Let $U/ND = x$, $[(\sigma/N)-1]^2 = b$, $p\pi = a$, and let α be a parameter between zero and unity; x, b and a are all positive quantities. The inequality (C 9) becomes

$$\alpha x = \frac{a^2}{[b/x^2 + a^2]^{\frac{1}{2}}}. \tag{C 10}$$

Solving (C 10) for b gives

$$b = (a^4x^4/\alpha^2)^{\frac{1}{3}} - a^2x^2 \tag{C 11}$$

or, with $y = a^2x^2$ and $\alpha^2 < 1{\cdot}0$,

$$b > y^{\frac{2}{3}} - y. \tag{C 12}$$

Then for the right-hand side a maximum, $b > \frac{4}{27}$, or $[(\sigma/N)-1]^2 > \frac{4}{27}$, and

$$(\sigma/N) > 1 + 2/(3\sqrt{3}).$$

It then follows that if the ratio of forcing frequency to natural frequency (σ/N) exceeds $1 + 2/(3\sqrt{3})$ the condition that U/ND should be greater than $1/\pi$ is relaxed to require only that U/ND be greater than zero.

Appendix D. Method of averaging solution to improve convergence

The expressions for vertical velcoity (w) created by the internal waves (e.g. equations (13), (19) and (21)) contain summations over p, where the vertical wavelength is $2D/p$. The sequence of p values often produces slowly convergent series with large contributions of alternating sign, and it is desirable to improve convergence. This is particularly important when small calculators (such as the HP-97 or the TI-59) are used in place of large computers. Averaging in the vertical direction is useful in such cases. Here we consider that the lift is distributed vertically over a distance $\pm\epsilon_1$ from the half-depth, $\frac{1}{2}D$, and that w is measured at a depth ϵ_2 below the free surface so that $-w(a-\epsilon_2)/\epsilon_2$ is an average dw/dz in the surface layer of thickness ϵ_2.

In (13)

$$w \sim \sin(bp\pi/D)\sin[(a-z)p\pi/D]. \tag{D 1}$$

With $b = D-a$ and $a = \frac{1}{2}D+\delta$, $-\epsilon_1 < \delta < \epsilon_1$ the vertical velocity w becomes

$$w(a-\epsilon_2) \sim \sin(\epsilon_2 p\pi/D)\frac{1}{2\epsilon_1}\int_{-\epsilon_1}^{\epsilon_1} \sin\left(\frac{p\pi}{2} - \frac{p\pi\delta}{D}\right) d\delta, \tag{D 2}$$

and the average dw/dz in the surface layer is

$$\frac{-w(a-\epsilon_2)}{\epsilon_2} \sim \frac{-\sin(\frac{1}{2}p\pi)\sin(\epsilon_1 p\pi/D)\sin(\epsilon_2 p\pi/D)}{\epsilon_2\epsilon_1 p\pi/D}. \tag{D 3}$$

If for simplicity we let $\epsilon_2 = \epsilon_1 = \epsilon$ then

$$\frac{-w(a-\epsilon)}{\epsilon} \sim -\sin\left(\frac{p\pi}{2}\right)\frac{\sin^2(\epsilon p\pi/D)}{\epsilon^2 p\pi/D}. \tag{D 4}$$

In the calculation of examples (D 4) replaces (D 1) in (13), (19) and (21).

Appendix E. Listing of non-dimensionalized equations used in calculations

Equations (13), (19) and (21) are presented as modified for computing the results appearing in this report. (The equations below are specialized to the case that

$$a = b = \tfrac{1}{2}D \quad \text{and} \quad x'_s = 0.)$$

Equation (13), multiplied by -2 and modified for computation, becomes†

$$\frac{-w(a-\epsilon)}{\epsilon}\frac{\bar{\rho}slD^2N\times 10^4}{2\pi F_0} = \sum_{m}^{\infty}\sum_{n}^{\infty} A_m A'_n \cos(K_1 x'/D)\cos(K_2 y/D)\times 10^4$$

$$\times \sum_{p}^{\infty}\frac{(-1)^{\frac{1}{2}(p+1)}\sin^2\left(\frac{\epsilon p\pi}{D}\right)\frac{f^2}{N^2}}{(p\epsilon^2\pi^2/D^2)}\left\{\frac{\sin\left[\left(\frac{f}{N}-\frac{UK_1}{ND}\right)N\tau-\frac{f}{N}Nt'\right]+\sin\left(\frac{f}{N}Nt'\right)}{\left(\frac{f}{N}-\frac{UK_1}{ND}\right)\left[1-\left(\frac{(\sigma/N)}{f/N-UK_1/ND}\right)^2\right]}\right.$$

$$\left.+\frac{\sin\left[\left(\frac{f}{N}+\frac{UK_1}{ND}\right)N\tau-\frac{f}{N}Nt'\right]+\sin\left(\frac{f}{N}Nt'\right)}{\left(\frac{f}{N}+\frac{UK_1}{ND}\right)\left[1-\left(\frac{(\sigma/N)}{f/N+UK_1/ND}\right)^2\right]}\right\}, \tag{E 1}$$

where

$$\left.\begin{aligned}\frac{f}{N} &= \left[1+\frac{p^2\pi^2}{K_1^2+K_2^2}\right]^{-\frac{1}{2}}, \quad \frac{\sigma}{N} = \frac{2\pi n'}{\tau N},\\ A_m &= \frac{2}{m\pi}\sin\left(\frac{m\pi l}{2L_1}\right) \quad \text{with} \quad A_0 = \frac{l}{2L_1},\\ A'_n &= \frac{2}{n\pi}\sin\left(\frac{n\pi s}{2L_2}\right) \quad \text{with} \quad A'_0 = \frac{s}{2L_2}.\end{aligned}\right\} \tag{E 2}$$

Equation (19) modified for computation becomes

$$\frac{-w(a-\epsilon)}{\epsilon}\frac{\bar{\rho}slD^2N\times 10^4}{2\pi F_0} = \frac{2}{\pi^2}\frac{D}{\epsilon}\sum_{\substack{1\\ p\,\text{odd}}}^{\infty}(-1)^{\frac{1}{2}(p+1)}\frac{\sin^2(\epsilon p\pi/D)}{(\epsilon p\pi/D)}\times 10^4$$

$$\times\int_0^{\infty}\frac{\sin(K_2 s/2D)}{K_2}\frac{f_c^2}{N^2}\frac{\sin(K_{1c}l/2D)}{K_{1c}}\frac{\cos(K_2 y/D)\cos(K_{1c}\xi/D)\,dK_2}{|(\partial(f/N)/\partial K_1)_{K_{1c}}-U/ND|} \tag{E 3}$$

and twice this for $\sigma = 0$. K_{1c} has two values for $\sigma \neq 0$ and one for $\sigma = 0$. All are defined by the iterative equation

$$K_{1c} = \frac{ND}{U}\left[\frac{1}{[1+p^2\pi^2/(K_{1c}^2+K_2^2)]^{\frac{1}{2}}}\mp\frac{\sigma}{N}\right]. \tag{E 4}$$

Also

$$f_c^2/N^2 = [1+p^2\pi^2/(K_{1c}^2+K_2^2)]^{-1}$$

and

$$\left(\frac{\partial(f/N)}{\partial K_1}\right)_{K_{1c}} = \frac{p^2\pi^2K_{1c}}{[1+p^2\pi^2/(K_{1c}^2+K_2^2)]^{\frac{3}{2}}[K_{1c}^2+K_2^2]^2}. \tag{E 5}$$

Note that U/ND must be greater than $1/\pi$ (unless $\sigma/N > 1+2/3\sqrt{3}$).

† After combining the arguments of the final sine-cosine product and summing positive and negative m values.

Equation (21) modified for computation becomes

$$\frac{-w(a-\epsilon)}{\epsilon}\frac{\bar{\rho}slD^2N\times 10^4}{2\pi F_0}=\left(\frac{2}{\pi}\right)^{\frac{1}{2}}\sum_{p\text{ odd}}^{\infty}\frac{(-1)^{\frac{1}{2}(p+1)}\sin^2(\epsilon p\pi/D)\,(\sigma/N)\times 10^4}{p(\epsilon^2\pi^2/D^2)\,(1-\sigma^2/N^2)}$$
$$\times\frac{\sin(\frac{1}{2}Ps\sin\theta)\sin(\frac{1}{2}Pl\cos\theta)}{\sin\theta\cos\theta}\frac{\cos(Pr-\frac{1}{4}\pi)}{(Pr)^{\frac{1}{2}}},\qquad\text{(E 6)}$$

with
$$PD=\frac{p\pi(\sigma/N)}{\sqrt{(1-(\sigma/N)^2)}}.\qquad\text{(E 7)}$$

Note that σ/N must be less than one for sustained waves.

Appendix F. A check on preferred directions

Others working in this field have usually employed stationary phase methods which lead to preferred directions. It seems desirable to show the relation of such work to the present analysis.

To investigate the possible appearance of preferred directions we first study w in a vertical plane normal to the flow direction. The parameters of example 2 are used ($\sigma/N=4$, $U/ND=5$) and the vertical plane is located behind the wing a distance $\frac{1}{2}\pi$ times the depth ($\xi/D=-\frac{1}{2}\pi$). Convergence problems arise for locations near the wing path so some averaging is necessary. Here w is averaged over a depth $\pm 0{\cdot}04D$ ($\epsilon/D=0{\cdot}04$) but the lift is fixed at $z/D=0$ (not distributed vertically as in the previous problems). Averaging smooths sharp peaks but does not eliminate them. In figure 10 the high local velocities induced by vortex lines left behind the wing can clearly be seen. This feature (which does not appear in the heaving problem studied by Rehm & Radt 1975) tends to obscure preferred directions. The simplest way to avoid this difficulty is to increase the wing span.

If we let the wing span approach ∞ ($s/D\to\infty$) and study a two-dimensional problem the numerical work is greatly reduced and no averaging is necessary. The lateral inclinations of the preferred directions are of course lost but the inclinations to the horizontal remain.

Consider the following examples in which no averaging is used ($\epsilon/D=0$), the oscillatory force has a frequency four times the natural frequency ($\sigma/N=4$), the observation line is vertical and behind the wing a distance $\frac{1}{2}\pi$ times the fluid depth ($\xi/D=-\frac{1}{2}\pi$). The velocity of the wing is 5·0, then 0·5, then 0·1 times the product of total depth and Brunt–Väisälä frequency ($U/ND=5{\cdot}0,\ 0{\cdot}5,\ 0{\cdot}1$). The quantity w^* is plotted against depth (z/D), where $w^*=w\pi\bar{\rho}lDN\times 10^4/4(F_0/s)$.

For $U/ND=5{\cdot}0$ (the value used for our previous moving wing cases) w^* decreases uniformly up to the free surface with no indication of preferred directions (see figure 11). For $U/ND=0{\cdot}5$ a rounded peak occurs near $z/D=0{\cdot}07$. For $U/ND=0{\cdot}1$ a sharp peak occurs at $z/D=0{\cdot}1$ with a secondary peak at $z/D=0$, and disturbances above $z/D=0{\cdot}1$ are small. The latter two cases resemble the results of Rehm & Radt (their figure 9) which show preferred inclinations to the horizontal of roughly 2 degrees to 6 degrees for σ/N (their ω/N) of 4.

REFERENCES

GRAHAM, E. W. 1973 Transient internal waves produced by a moving body in a tank of density-stratified fluid. *J. Fluid Mech.* **61**, 465–480.

HENDERSHOTT, M. C. 1969 Impulsively started oscillations in a rotating stratified fluid. *J. Fluid Mech.* **36**, 513–527.

MOWBRAY, D. E. & RARITY, B. S. H. 1967 A theoretical and experimental investigation of the phase configuration of internal waves of small amplitude in a density stratified liquid. *J. Fluid Mech.* **28**, 1–16.

PHILLIPS, O. M. 1969 *The Dynamics of the Upper Ocean*. Cambridge University Press.

REHM, R. G. & RADT, H. S. 1975 Internal waves generated by a translating oscillating body. *J. Fluid Mech.* **68**, 235–258.